10-1-2011

Glitter and Glints on Water

David K. Lynch

David S. P. Dearborn

James A. Lock
Cleveland State University, j.lock@csuohio.edu

Original Citation

Lynch, David K., David S. P. Dearborn, and James A. Lock. "Glitter and Glints on Water." *Applied Optics* 50 (2011): F39-F49.

Glitter and glints on water

David K. Lynch,[1,*] David S. P. Dearborn,[2] and James A. Lock[3]

[1]Thule Scientific, P.O. Box 953, Topanga, California 90290, USA

[2]Lawrence Livermore National Laboratory, Livermore, California 94550, USA

[3]Department of Physics, Cleveland State University, Cleveland, Ohio 44115, USA

*Corresponding author: thule@earthlink.net

Received 10 May 2011; accepted 8 July 2011;
posted 21 July 2011 (Doc. ID 147119); published 30 August 2011

We present new observations of glitter and glints using short and long time exposure photographs and high frame rate videos. Using the sun and moon as light sources to illuminate the ocean and laboratory water basins, we found that (1) most glitter takes place on capillary waves rather than on gravity waves, (2) certain aspects of glitter morphology depend on the presence or absence of thin clouds between the light source and the water, and (3) bent glitter paths are caused by asymmetric wave slope distributions We present computer simulations that are able to reproduce the observations and make predictions about the brightness, polarization, and morphology of glitter and glints. We demonstrate that the optical catastrophe represented by creation and annihilation of a glint can be understood using both ray optics and diffraction theory.

OCIS codes: 010.0280, 010.7295, 080.1235, 330.5000, 330.6790, 010.4450.

1. Introduction

> "Water, whether still or in motion, has so great an attraction for the lover of nature, that the most beautiful landscape seems scarcely complete without it. There are no effects so fascinating as those produced by the reflexions in nature's living mirror, with their delicacy of form, ever fleeting and changing, and their subtle combinations of colour." M. Montagu-Pollock *Light and Water: A Study of Reflexion and Colour in River, Lake and Sea*, 1903 [1]

That sparkling patch of sunlight (or moonlight) reflected on the ocean is known to all (Figs. 1 and 2). Variously called the *sun streak* [1], the *road to happiness* [2], the *golden bridge* [3], and the *glitter path* [4], it appears as a bright, elongated patch of light on the water and is composed of countless glints that appear and disappear faster than the eye can follow. As a result, glints seem to blink on and off, apparently at random.

In this paper, we shall use the term *glitter* to refer to the entire field of individual specular reflections, the latter being called *glints*. We will also refer to the sun as the light source, even though the moon, stars, and even clouds can be the light source for glitter.

Glitter would seem to be little more than specular reflections of the sun, for we see what appear to be static analogs of it on ice, in grass and spider webs, and in ice crystal halos like subsuns and pillars [5]. As we will see, however, glitter is formed in a complicated way, while many of the so-called analogs are based on simple glints from flat surfaces or surfaces that do not move.

With rare exceptions, glitter is symmetric about the vertical plane containing the sun and the observer. When the sun is high, glitter is elliptical (Fig. 1) and grows gradually more elongated and narrower as the sun elevation decreases. Eventually the distant end of the glitter is truncated by the horizon (Fig. 2). When the sun is very low, the glitter has the same width as the sun and appears as a vertical stripe on the water directly beneath the sun and extending to the horizon. By the time the sun reaches

0003-6935/11/280F39-11$15.00/0

Fig. 1. (Color online) Elliptical high sun glitter (ocean).

the horizon, the glitter has almost always disappeared because waves can block the nearly horizontal reflections, which are already faint because of the near-infinitesimally small areas for reflection from the tops of the waves. If there are variations in the slopes of the waves across the glitter, it will show broader or narrower widths. In the case of a flat patch of water, glitter will disappear altogether.

The peak intensity of the glitter occurs in the center of the ellipse. The center of the ellipse, however, does not fall where the specular point would be on the same flat sea, but rather is shifted toward the horizon [6], an effect common to reflection from any rough surface [7].

The first comprehensive treatment of glitter was by Montagu-Pollock [1]. Hulburt [8] worked out the geometry of glitter as it relates to sun elevation and wave slope, but did not consider the detailed optics of single glints. Soon after Hulburt's work, Minnaert reported seeing "closed coils of light" in water at night from reflected street signs [6]. Later investigations by Cox and Munk [9,10] that extended Hulburt's work produced quantitative and statistical results about glitter that have been used in many areas of remote sensing.

A time exposure of glitter where the glints are resolved shows a field of complex but always closed loops (Fig. 3). This surprising morphology was predicted theoretically by Longuet-Higgins and collaborators [11–13] before it was explicitly observed and recognized. As the wave passes, a single glint appears, brightens, splits into two separate glints that move around the surface before coming back together, brightening and then vanishing, all in a fraction of a second (Fig. 4, single image from Media 1). Longuet-Higgins called them "twinkles" and termed the process "creation and annihilation" (C/A). C/A is completely reversible in time and represent the same optical process. So common are these closed loops that they can be easily seen even by day—if specifically sought—in any rippled water surface like puddles, ponds, swimming pools, and cups of coffee, that reflect small, pointlike light sources.

The trajectories of glint pairs computed by Longuet-Higgins were based on monochromatic water waves. In reality, however, the sea surface consists of a broadband spectrum of deep (dispersive) and shallow (nondispersive) water gravity waves, and capillary (surface tension) waves. This results in extremely complex tracks, though they still are closed, or mostly so (Fig. 3).

Despite the firm observational and theoretical foundation for understanding glitter and glints, there are a number of aspects that have not been explained: What role do capillary waves play in glitter

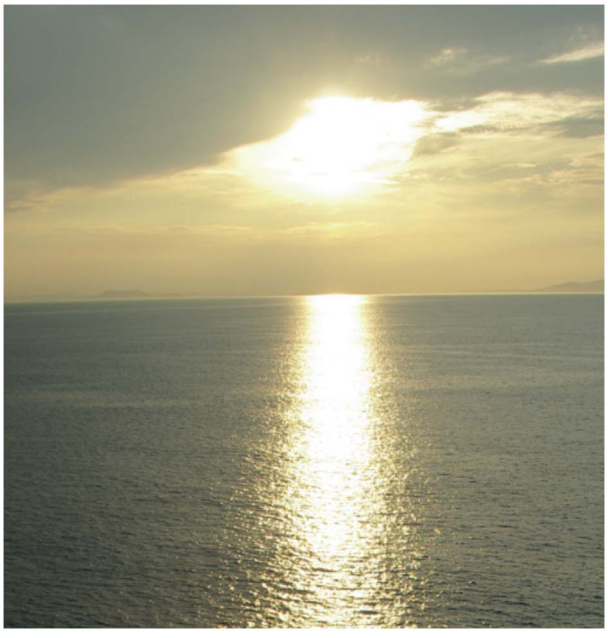

Fig. 2. (Color online) Elongated low sun glitter reaching to the horizon (ocean).

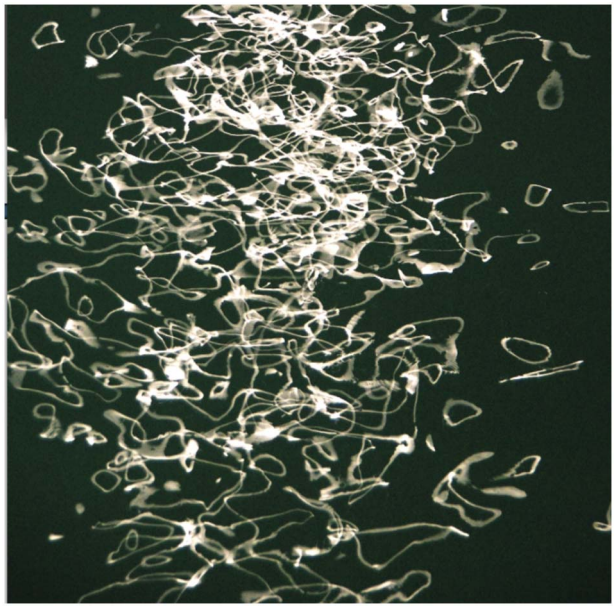

Fig. 3. (Color online) 4 s exposure of moon glitter showing myriad closed trajectories of the glints (ocean).

Fig. 4. (Color online) Single frame from a 1000 fps movie showing glint evolution and morphology (bucket).

formation? Is glitter in deep water different from that in shallow water? Why is the occasional glitter bent or tilted out of the vertical plane? Is glitter affected by sky conditions?

In this paper, we investigate glitter and glints based on short and long time exposure photographs and high frame rate videos. Both the sun and moon were used as light sources for the ocean and in tubs of water in the laboratory. We also modeled the time and geometrical behavior of glints using both computer simulations and analytic methods. Building upon the foundation provided by the authors cited above, we extend the analysis of glint morphology and time behavior and demonstrate how individual glints contribute to form the larger, unresolved glitter path. Computer simulations provide validation and prediction.

2. Observations

A. Still Photographs

Glints change so rapidly that visual observations are insufficient to provide little more than qualitative understanding. Therefore, we took still photographs and high-speed videos (1000 fps (frames per second)). Two bodies of water were the main source of glitter: the ocean viewed from piers in Santa Monica Bay (California), and a large plastic tub of water in which the authors made waves by "kicking the bucket." Despite their seeming differences, both bodies of water produced identical glitter phenomenology.

Glints are not randomly distributed over the glitter, but rather occur in relatively isolated groups, which sometimes contain dozens of glints, often arranged in linear formations like beads on a necklace (Figs. 5 and 6). These are due to capillary waves (surface tension waves) and can represent the majority of glints. A raft of capillary waves typically has 5–10 waves and thus produces 5–10 times as many glints as the gravity waves upon which it rides.

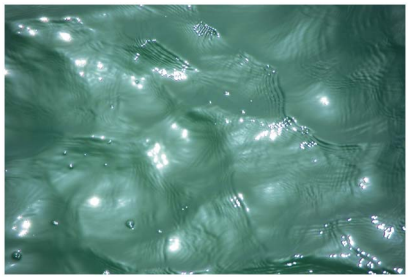

Fig. 5. (Color online) High sun glitter resolved. The individual glints are not randomly distributed but cluster together, primarily in capillary wave groups (ocean).

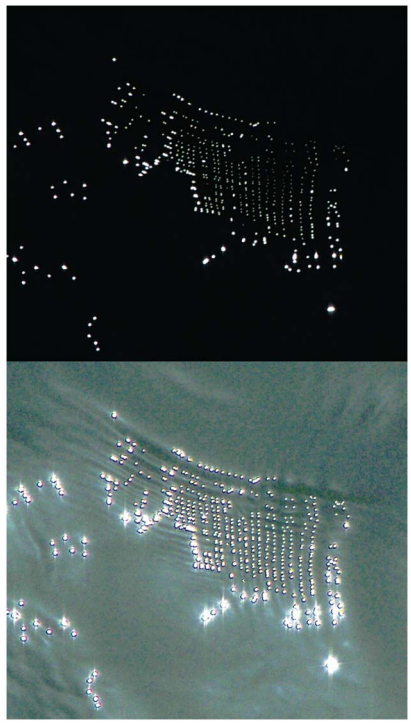

Fig. 6. (Color online) Top: image of resolved glitter adjusted to show only the glints. Bottom: same image adjusted to show the glints and the water's surface (ocean).

Also shown in Figs. 5 and 6 are a number of static glints. These are due to reflections and refractions from air bubbles on the surface, parts of which are oriented just right to reflect sunlight to the observer. Such glints are long-lived, vanishing only when the bubble pops. They usually do not make a significant contribution to the glitter in either brightness or number of glints.

At the instant of C/A, the glints suddenly flash brightly (Fig. 7). Longuet-Higgins [11] attributes this to the finite angular diameter of the sun in which the specular reflection momentarily broadens and thus reflects more light to the observer. While this unquestionably occurs, we wonder what role, if any, constructive interference plays in forming the flash. In a C/A pair, each glint comes from a slightly different

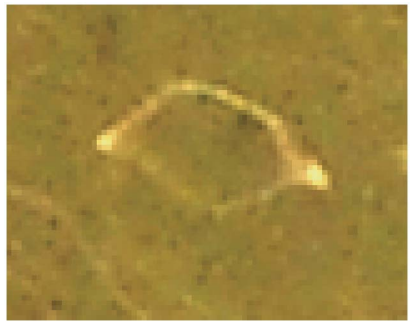

Fig. 7. (Color online) Close-up time exposure of a loop showing the C/A flashes at the cusps (bucket).

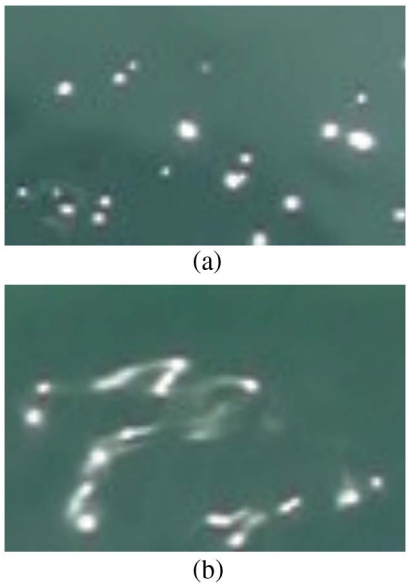

(a)

(b)

Fig. 8. (Color online) High frame rate glitter morphology: (a) clear sky, (b) hazy sky with a bright solar aureole (bucket).

ray. As one glint approaches another, the phase difference between rays decreases until just before they merge, at which time the two rays are in phase and thus might constructively interfere.

Small, distinct and crisp glints are most visible when the sky is clear [Fig. 8(a)]. If the sun is viewed through even very thin clouds or haze, light from the aureole combines with direct sunlight to produce broader, fuzzier glints [Fig. 8(b)]. This is equivalent to making the sun larger, thus spreading out its effects in the reflections. Even though the centers of each member of the pair may be well separated, the increased angular width of the apparent sun leaves them broader and with longer tails that may not completely separate.

B. High Frame Rate Movies (1000 fps)

Figure 9 shows a selected sequence of frames from a high-speed movie that reveals the time history of one loop's life. The C/A brightening discussed by Longuet-Higgins [11] occurs because, as the newly created glint begins to split, its surface area momentarily increases. After it has split in two, the glints return to their original size and the average brightness decreases, remaining relatively constant until it brightens once again as the pair merges, brightens, and vanishes.

Pairs are created in less than a millisecond and similarly vanish on the same time scale. Glints lifetimes from creation to annihilation vary from less than 1 ms to up to about 0.01 s, depending on the speed, wavelengths, and slopes of the waves.

Online Media 1 (static frame Fig. 4 from Media 1) is a digital video of sun glitter on a clear day in a bucket made with a frame rate of 1000 fps. In watching the glints scurry around, one is not able to tell the direction of time; running the movie backwards is indistinguishable form running it forward (Fig. 10,

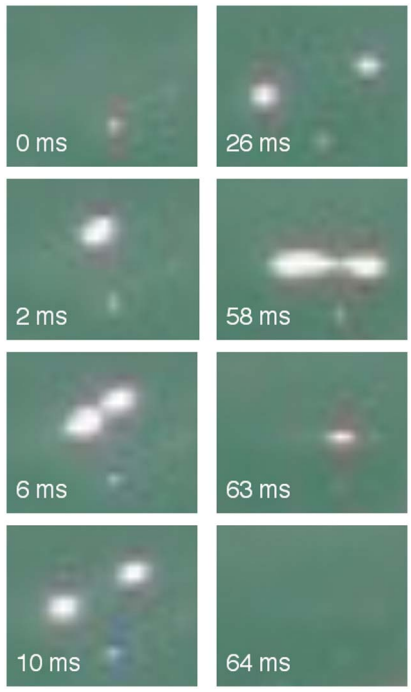

Fig. 9. (Color online) High frame rate (1000 fps) time sequence of loop evolution in a bucket showing C/A in less than 1 ms. The faint static glint near bottom center of each frame is due to a bubble.

single frame from Media 2). Waves are continuous, so creation and annihilation are simply time-reversed versions of each other.

Creation occurs in pairs, but before the two glints recombine, the individual glints may themselves split, and these daughter pairs can split again. Sometimes 4, 6, 8, 10… glints progressively pop out in a line almost instantaneously and evolve from there. Annihilation occurs similarly, 8, 6, 4, 2 pairs come together, flash, then vanish. It is often hard to measure the lifetime of a single glint because when it splits into two, three, four, or more pairs, its identity as a single glint is lost. Sometimes, a single glint will appear, then vanish without splitting. We believe that this is simply two pairs that form and disappear without moving far enough apart to be resolved.

The two members of a pair do not always recombine with each other (Fig. 11, single frame from Media 3). Sometimes, one member will run off and join with another apparently unrelated glint in annihilation. The glints seem to "know" about each other, choosing some glints to annihilate with and avoiding others, even those nearby.

Fig. 10. (Color online) Single frame from 1000 fps Media 2. This shows a single C/A event near the center of the frame. The direction of time is reversible (bucket).

Fig. 11. (Color online) Single frame from 1000 fps Media 3 showing two glints from different C/A events that recombine and vanish (lower right side of the frame) (bucket).

3. Computer Simulations

A number of computer programs were developed to study the general wave properties leading to observable glint behavior. These programs were used to model aspects of glitter and glints as viewed on various surfaces (planar or spherical as from a satellite), and with different waveforms. An arbitrary number of waves were either user specified or constructed from a Joint North Sea Wave Project (JONSWAP) spectrum of ocean waves [14]. Slope distributions were examined and compared to observed distributions [9,10]. The wave shapes could be either simple sinusoids or Fourier constructs. For deep water waves, each wave moves at its own speed as determined by the dispersion relation. The sun's angular diameter was fixed at 0.5 degrees, and its position on the celestial sphere was specified. Observer position was fixed for studies on the detailed behavior of glints, but may also include a time-varying camera position and orientation. The view is drawn with an elementary lens transform, and crests of waves may occult more distant waves. For simplicity, we always used a geometry where the observer could see every point on the water's surface, i.e., nothing was hidden behind other wave crests. Real physical units (SI) were used throughout.

Glints were modeled with simple geometrical optics that included Fresnel reflectivity and polarization. The output was in the form of simulated images, or QuickTime movies, showing either the glint location or the time-integrated glint tracks (Fig. 12, single frame from Media 4). By selecting the angular field of view, it was possible to zoom in on a single glint or zoom out and model the entire glitter, including very distant (satellite) views of glitter on the surface of the spherical Earth.

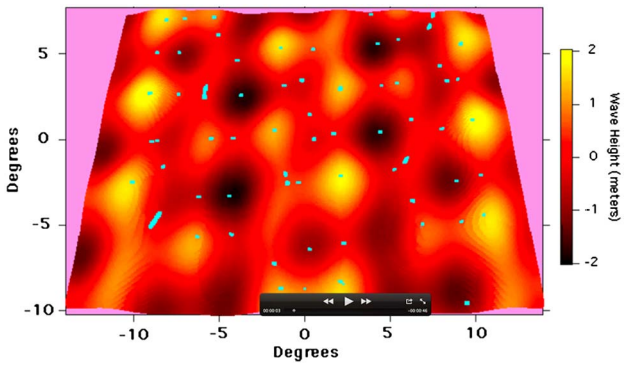

Fig. 12. (Color online) Single frame from simulation movie (Media 4). The small dots show the locations of the glints. Amplitude of the waves is shown by the color scale at the right. Computational parameters were solar elevation, 45°; solar diameter, 0.5 field; degrees size on the water, 200 m × 200 m; and observer distance from the center of the frame, 200 m. Four deep water traveling waves were used, each of amplitude 0.5 m with arbitrary phases. Wavelengths were 50, 40, 30, and 20 m.

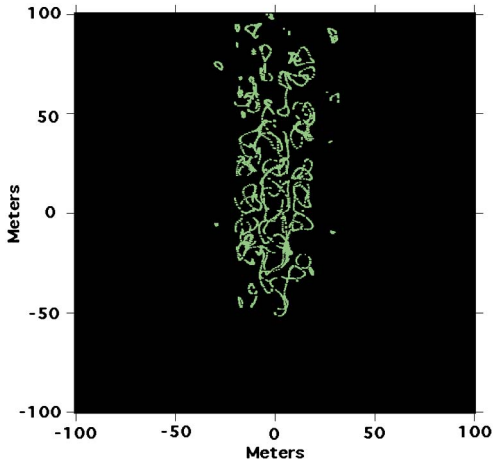

Fig. 13. (Color online) Theoretical computation of glitter showing time-integrated glint tracks forming closed loops.

Figure 13 shows a simulation in which the glint's location is recorded as a trail of light. Each glint pair traces out a closed loop, like those shown in Fig. 3. Open loops are those where the calculation started or stopped before the loop was completed and the pairs were still separated. There is no discernible difference in our simulations of C/A and loop morphology between deep (dispersive) and shallow (nondispersive) water waves.

4. Analysis

A. Creation and Annihilation

C/A represents an optical fold catastrophe in bifurcation theory [15,16]. A catastrophe is sudden shifts in a system's behavior arising from small changes in

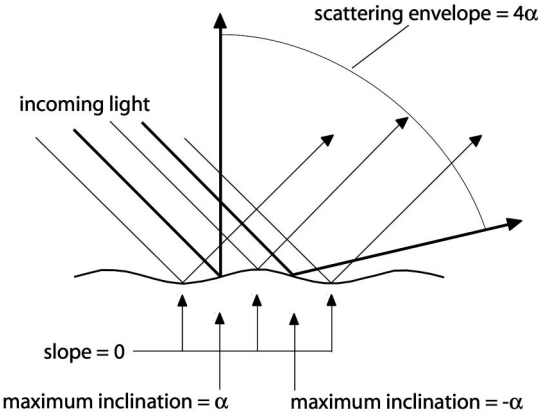

Fig. 14. Geometry of glitter formation illustrated using a monochromatic sinusoidal wave in one dimension and a point source of light. At any instant, light reflected from one complete wavelength will be scattered into a finite range of angles corresponding to four times the inclination angle of the steepest part of the wave.

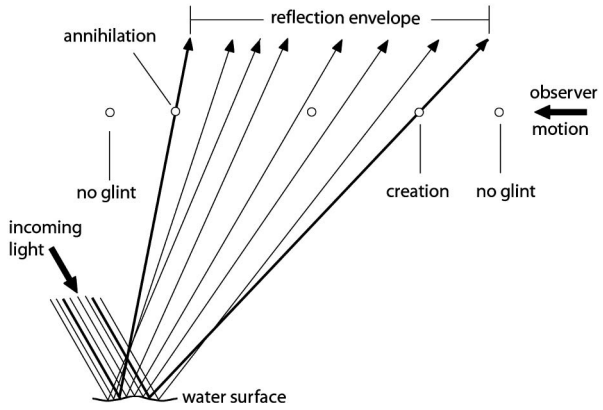

Fig. 15. Instantaneous C/A of glints can be understood by an observer passing through the reflection envelope from right to left. While outside the envelope (far right), no glint is seen. When the observer reaches the edge of the envelope, the glint first appears, i.e., creation takes place. As the observer enters the envelope, the glint splits in two. While inside the envelope, two glints are seen (see Fig. 9). As the observer approaches the opposite side of the envelope (left), the two glints come together, then disappear when the observer reaches the edge of the envelope (annihilation).

circumstances. In this case, the catastrophe is the sudden appearance and disappearance of the glint.

C/A can be understood geometrically in terms of ray bundles (Fig. 14). We will discuss the simplest case of light reflected in the vertical plane containing the observer and light source, though the more general three-dimensional case follows by obvious extension. Consider a distant, point source of light that illuminates a continuous water surface whose maximum inclination is α. Light is reflected into an envelope whose angular with is 4α. All rays reflected from other parts of the wave are within the envelope's extreme angles. Depending on the local wave curvature, the reflected light may form a real or virtual image of the light source.

For convenience, we replace the moving wave and static observer by a static wave and a moving observer. When the observer is outside the envelope, no glint is seen. As soon as the observer touches the envelope, a glint appears, and it originates from the steepest part of the wave (Fig. 15). Once inside the envelope, the observer will see two glints, one from the near side and one from the far side of the wave (Fig. 16). This happens as the newly created

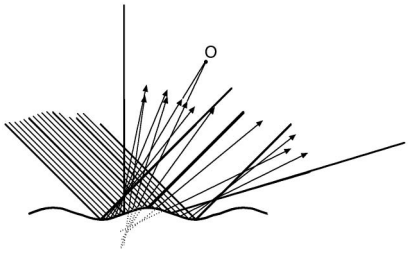

Fig. 16. When inside the reflection envelope, two glints are seen by the observer O because from one wavelength on a smooth monochromatic surface, there will always be two and only two rays that reach the observer. One image is real and the other is virtual.

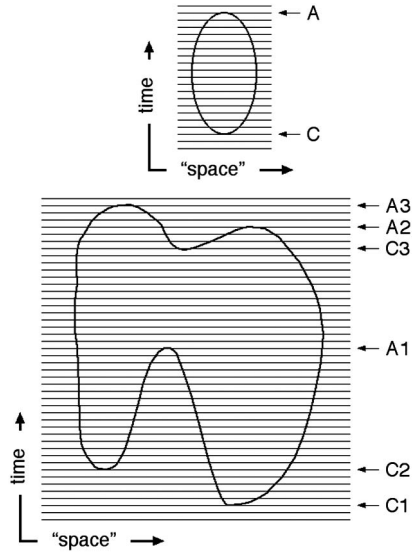

Fig. 17. C/A can be understood in terms of a closed manifold in space–time where glints occur at the intersection of a horizontal "time line" and the closed curve. Time runs from bottom to top. Upper: If the time line does not intersect the curve, no glints are seen. When it reaches the curve and is tangent to it, creation occurs. At later times, two intersections occur so two glints are seen. Annihilation occurs in the reverse process. Lower: When the manifold is more complex, more complex behavior is seen. Here two creation events (C1 and C2) (lower two lobes of the manifold) produce two glint pairs (four intersections). As time progresses, single glints from different pairs merge to produce an annihilation (A1) near the center of the manifold, thus leaving two "unpaired" glints at the extreme left and right of the manifold. A third creation happens at C3, producing another pair of glints that separate. Then, each member of the newly created pair joins with one of the two outer glints and two more annihilations occur (A2 and A3). The manifolds—even when quite complex—represent the continuity of the surface. Being closed loops themselves, they can explain in a simple way the complex glint behavior seen in the media.

glint splits in two, each daughter glint then moving away from the location of maximum slope, one moving up the wave toward the crest, the other moving down the wave toward the trough.

Fig. 18. (Color online) Bent or tilted glitter occurs when there is an asymmetric distribution of waves slopes. The most common occurrence is when wind blows continuously from one direction but can also occur when a wave whose wavelength is large compared to the observed glitter path encroaches on glitter produced by much smaller wavelength waves. In this picture, the long bow wave from a ship slides under the ambient short waves, causing them to be tilted more in one direction than the other (ocean).

Fig. 19. (Color online) Bent glitter simulated by our theoretical code. Wave slopes in the background are uniformly distributed but those in the foreground have been skewed, thereby making the glitter deviate from the vertical plane containing the sun and observer.

This sequence of events represents the sudden appearance (creation) and splitting of the glint. When the observer reaches the opposite envelope, the two glints rejoin and disappear (annihilation) as the observer moves outside the envelope. Obviously, the process is time reversible.

The geometrical argument above can be more elegantly expressed using Huygens' diffraction theory. Lock and Adler [17] have done this for rainbows and their methods are applied to glints in Appendix A. A useful visualization based on their approach is shown in Fig. 17. Here the glints are defined by the intersection of the horizontal "time" lines with the glint manifold. The horizontal axis is a generalized spatial coordinate and the vertical axis is time. The upper figure shows the C/A for a simple loop. Starting at the bottom and moving up time line by time line, we see that at first there is no glint because the time line does not intersect the loop. Soon a creation event occurs when the time line is tangential to the loop, followed by splitting into two glints, i.e., the horizontal time line intersects the loop at two places.

Fig. 20. (Color online) Glitter observed from space. The optical signature of glitter from oceans on extrasolar planets might be detectable from Earth, thereby providing a way to search for such planets. (Photograph courtesy of NASA).

Fig. 21. (Color online) When the sun is replaced by an extended source of light like sky, clouds, and mountains, glitter blossoms into a complex field of graceful loops and swirls. These structures are formed in exactly the same way as pointlike glints, but exhibit a vastly richer morphology, just as a sky full of clouds is more complex than a single sun (ocean).

The two glints move around and eventually approach each other, finally coalescing and vanishing (A). The lower figure shows a more complex situation whereby two apparently independent creation events occur. One glint from one pair "finds" one glint from the other pair and the two annihilate. In all cases, there is an even number of glints (0, 2, 4…) and the same number of C and A events. A more rigorous description of the process is given in Appendix A.

B. Bent and Tilted Glitter

From time to time, photographs appear that show glitter that is bent, curved, or has a portion that is not in the vertical plane (Fig. 18). It seems obvious that such features are the result of waves whose transverse profiles (left-right relative to vertical) are asymmetric.

One possible way is to have a field of short-wavelength glitter-producing waves overtaken by a long wavelength wave. We believe that this causes the short-wavelength waves to be tilted one way or the other on average. As a result, the wave slope distribution is shifted in one direction, thereby shifting the glitter sideways. This is the case in Fig. 18, where the long bow wave of a ship moves into a field of glitter.

Another way to produce asymmetric wave slopes is with wind. Wind blowing across water will produce all wavelengths of waves, starting with short waves (capillary waves—"cat's paws") and building longer wavelengths as time goes on. Wind waves tend to

Fig. 22. (Color online) Computer simulation of reflections from a scene with sky, clouds, and mountains.

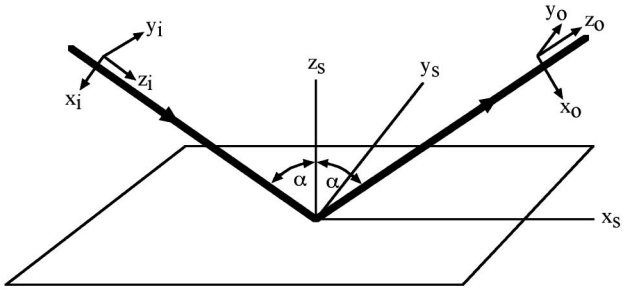

Fig. 23. Coordinate systems of the incident plane wave (i), a flat horizontal surface (s), and the wave specularly reflected from the flat surface to the observer (o). The actual rippled reflecting surface is given by z_s as a function of x_s and y_s and lies alternately above and below the x_s, y_s plane.

have smaller slopes on the windward side and larger slopes (steeper) on the leeward sides. The result is an asymmetric slope distribution, which leads to bent glitter, modeled in Fig. 19.

5. Discussion

Not all seas show capillary waves, but most do. Indeed, the Beaufort Wind Force Scale lists capillary waves (ripples) as being present in every wind condition except Beaufort Scale 0, i.e., "calm." Having spent a great deal of time gazing at the ocean from the shore, piers, and boats, we confirm that capillary waves are virtually always part of an ocean wave spectrum.

Wind produces capillary waves by directly shearing the water's surface forming Kelvin–Helmholtz instabilities. Ripples are also produced by droplets splashing on to the water's surface, popping bubbles, breaking waves, waves reflecting off a wall or piling, or virtually anything that locally disturbs the surface. There is also a nonlinear process by which

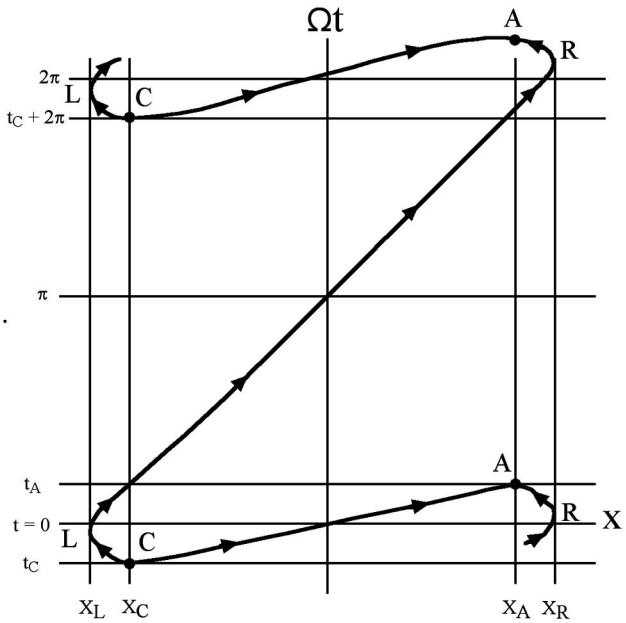

Fig. 24. Trajectories of alternately one or three glints as a function of time between the creation (C) and annihilation (A) events.

gravitational energy from gravity waves can be converted into surface tension waves [18–20]. We think this effect is not significant enough to explain the almost ubiquitous occurrence of capillary waves that we see, because the mechanism is most efficient for steep water gravity waves.

Sun glints are very bright, usually saturating the eye, film, and any electronic sensor. Indeed, staring at sun glitter from close range where individual glints are well separated produces dark, pointlike after-images. Being distorted images of the sun diminished only by Fresnel reflectivity and atmospheric scattering and absorption, glitter is readily visible from space (Fig. 20). As such, glitter is the brightest incoherent light coming from the Earth. Recently, Williams and Gaidos [21] argued that starlight glittering off extrasolar planets could be bright enough to detect.

For the visual observer of glitter, the sun is effectively a point source. If we replace small light sources such as the sun and aureole by a bright sky-filling structured source (clouds, mountains, sky, etc.), the surface reflections blossom into a complex field of beautiful, dancing color, all showing the characteristic closed loops and rounded, oval patterns (Fig. 21). They have been reported by many observers (e.g., [22,23] and have been simulated by our code (Fig. 22).

6. Conclusions

We have investigated the detailed and collective phenomenology of sunlight reflected from a wavy water surface. Capillary waves were found to be the largest source of light in glitter. When thin clouds are present, the resulting solar aureole broadens the glints, though the overall glitter appears no different from that produced in a clear sky. High-speed movies (1000 fps) reveal an astonishing variety of glint behavior, demonstrating that a continuously curved surface produces glints whose position and movement are not random, but which are correlated in sometimes surprisingly complex ways. The optical catastrophe representing C/A of glints may be understood using both ray optics and diffraction theory. Asymmetric wave distributions can produce glitter with unusual shapes. The most general case of an extended light source results in a continuum of graceful, colored shapes, fully analogous with the closed loops formed by near-pointlike light sources.

The authors appreciate almost 40 years of collaboration with Bill Livingston on many aspects of light, color, and astronomy, including glitter. Lawrence S. Bernstein and Rafael Panfili of Spectral Sciences, Inc. provided useful discussion and support.

Appendix A

In this appendix, we outline a derivation of the various features of the glints observed in Fig. 8 and in Media 3 using wave optics methods in the context of catastrophe theory. Consider a plane wave of field

strength E incident at an angle α on a rippled reflecting surface above the horizontal plane as in Fig. 23. In the x_i, y_i, z_i coordinate system of the incident plane wave, the plane wave propagates in the positive z_i direction and the surfaces of constant phase are parallel to the x_i, y_i plane. The shape of the rippled surface is taken to be z_s as a function of x_s and y_s with respect to the horizontal coordinate system in the figure. An observer is located in the specular reflection direction of the incident plane wave for a perfectly flat reflecting surface as in Fig. 23, and he detects the light reflected from the rippled surface on his viewing screen. The viewing screen is the x_o, y_o plane of the observer's x_o, y_o, z_o coordinate system, and the origin of the viewing screen is a diagonal distance $|z_o|$ from the origin of the x_s, y_s, z_s coordinate system.

A small patch of the plane wave strikes the reflecting surface at the location x_s, y_s, z_s at the time t_s, and a small patch of the wave reflected from this location arrives at the observer at the time t_o. The reflected field arriving at x_o, y_o, z_o at the time t_o is the superposition of the reflected waves leaving the surface z_s at all locations x_s, y_s at the appropriate retarded time t_s. In order to determine the reflected wave, one first converts the phase of the electric field of the plane wave from the x_i, y_i, z_i coordinate system to the x_s, y_s, z_s coordinate system of the surface. In order to determine the retarded time difference $t_o - t_s$ from any position on the reflecting surface to any location on the observer's viewing screen, one converts the location on the reflecting surface from the x_s, y_s, z_s coordinate system to the x_o, y_o, z_o coordinate system. Following this procedure, assuming that α is far from grazing incidence, and that the reflecting surface has a small slope, the reflected electric field reaching the viewing screen is [24]

$$E_o(x_o,y_o,t_o) = -[ikE\cos(\alpha)/(2\pi z_o)]\exp[i(kz_o - \omega t_o)] \times \int dx_s \int dy_s \exp[ik\Phi(x_o,y_o,x_s,y_s)], \quad \text{(A1)}$$

where the phase function Φ is

$$\Phi(x_o,y_o,x_s,y_s) = -2z_s\cos(\alpha) + [x_o - x_s\cos(\alpha)]^2/(2z_o) + (y_o - y_s)^2/(2z_o), \quad \text{(A2)}$$

plus higher order terms that will hereafter be neglected. The second and third terms of Eq. (A2) describe Fresnel diffraction of the reflection of the incident plane wave from the perfectly flat x_s, y_s plane, and the first term gives the extra path length of the reflected wave due to the height of the rippled surface above the x_s, y_s plane.

In this appendix, we consider the simple one-dimensional example of light reflected from a single sinusoidal traveling wave of amplitude A, wavenumber K, frequency Ω, and propagating in the positive x_s direction

$$z_s = -A\cos(Kx_s - \Omega t). \quad \text{(A3)}$$

We consider the reflected light at the origin of the viewing screen $x_o = y_o = 0$. For this case, Eq. (A2) reduces to

$$\Phi(x_s,t) = 2A\cos(\alpha)\cos(Kx_s - \Omega t) + x_s^2\cos^2(\alpha)/(2z_o) + y_s^2/(2z_o). \quad \text{(A4)}$$

In particular, we are interested in the observer looking at the moving sinusoidal reflecting surface and seeing the glint or glints of the incident plane wave that propagate from the surface to his eye, which is at the origin of the viewing screen. These glints correspond to the stationary phase point or points of the phase integral of Eqs. (A1) and (A2),

$$\partial\Phi/\partial x_s = 0 = -2AK\cos(\alpha)\sin(Kx_s - \Omega t) + x_s\cos^2(\alpha)/z_o. \quad \text{(A5)}$$

This equation can be simplified by considering the changes of variables

$$X = Kx_s, \quad \text{(A6)}$$

$$u = X - \Omega t, \quad \text{(A7)}$$

$$M = \cos(\alpha)/(2AK^2z_o), \quad \text{(A8)}$$

$$N = (1 - M^2)^{1/2}/M, \quad \text{(A9)}$$

giving

$$M(u + \Omega t) = \sin(u). \quad \text{(A10)}$$

The solutions of Eq. (A10) give the observed positions X of the glints on the reflecting surface as a function of time t. Although Eq. (A10) may be solved numerically for all times, certain significant features of the glints become manifest if we solve the equation analytically in the vicinity of certain special times, namely the glare spot C/A events. It should be pointed out that the annihilation event subscript A appearing below is not to be confused with the amplitude of the sinusoidal wave of Eq. (A3), which is also denoted by A.

Geometrically, the left side of Eq. (A10) when graphed as a function of u for various values of t is a sequence of parallel diagonal straight lines, all having slope M. The right side of the equation is an unmoving sine curve of unit height. The solution(s) of the equation for a given time is (are) the intersection(s) of one of the diagonal straight lines with the sine curve. When $M > 1$, there is only one intersection point for each t. The existence of a single glint that moves back and forth as the wave passes by corresponds via Eq. (A8) to the observer's distance from the surface z_o being relatively small, i.e., $z_o < 1/(2AK^2)$ for $\cos^2(\alpha) \approx 1$. On the other hand, Eq. (A10)

has either one or three solutions, depending on the value of t, when $2/(3\pi) < M < 1$. This regime corresponds to the observer being higher above the reflecting surface, $1/(2AK^2) < z_o < 3\pi/(4AK^2)$. For yet smaller values of M or larger values of z_o, Eq. (A10) has five or more solutions corresponding to the observer seeing an increasingly large number of glints as he moves farther away from the surface [12]. For the rest of this appendix, we analyze the case $1/(2AK^2) < z_o < 3\pi/(4AK^2)$, or, equivalently, $0 < N < 4.605$, where the observer sees a temporal evolution between one and three glints as is the case in Media 3.

The glint C/A events occur when Eq. (A10) is satisfied and when the slopes of the left and right sides of Eq. (A10) are equal, i.e.,

$$M = \cos(u). \tag{A11}$$

In the geometric interpretation of this situation, one of the diagonal straight lines just touches the sine curve and is tangent to it, giving a double solution [24]. If the diagonal straight line is moved in one direction, it no longer intersects the sine curve. But if it is moved in the other direction, the double solution splits into two distinct solutions. The solution of Eqs. (A10) and (A11) is

$$\Omega t = \tan(u) - u, \tag{A12}$$

or, equivalently,

$$X_{A,C} = \pm N, \tag{A13a}$$

$$t_{A,C} = \pm[N - \operatorname{arc}\tan(N)]/\Omega, \tag{A13b}$$

where the plus sign corresponds to the annihilation event and the minus sign corresponds to the creation event. In the vicinity of the annihilation event, we let

$$X = X_A \pm \delta, \tag{A14}$$

where $\delta \ll 1$. Substituting Eq. (A14) into Eq. (A10) and a Taylor series expansion in powers of δ, we obtain

$$\Omega t = \Omega t_A - N\delta^2/2 + O(\delta^3), \tag{A15}$$

or, equivalently,

$$t \approx t_A - N(X - X_A)^2/(2\Omega). \tag{A16}$$

This behavior is shown in Fig. 24 and illustrates that as the two glints approach the annihilation event from opposite directions, their velocities dX/dt become infinite [11]. Following a similar derivation in the vicinity of the creation event, one obtains

$$t \approx t_C + N(X_C - X)^2/(2\Omega). \tag{A17}$$

Figure 3 is an example of the evolution illustrated in this figure for the case of an even number of glints.

Since the two glints approach the annihilation event from opposite directions, the extremum position of the rightmost glint (R) before the annihilation event is given by $dX/dt = 0$, or, equivalently, $dt/dX \to \infty$. Taking the derivative of Eq. (A10), this occurs for

$$X_R = (N^2 + 1)^{1/2}, \tag{A18a}$$

$$t_R = [(N^2 + 1)^{1/2} - \pi/2]\Omega. \tag{A18b}$$

Similarly, the extremum position of the leftmost glint (L) after the creation event is

$$X_L = -X_R, \tag{A19a}$$

$$t_L = -t_R. \tag{A19b}$$

In the vicinity of the extremum position of Eq. (A19a), we let X be of the form

$$X = X_L + \delta, \tag{A20}$$

where $\delta \ll 1$. Substituting Eq. (A20) into Eq. (A10) and a Taylor series expansion in powers of δ, one obtains

$$\delta \approx (N^2 + 1)^{1/2}\Omega^2(t - t_L)^2/2, \tag{A21}$$

or, equivalently,

$$X \approx X_L + (N^2 + 1)^{1/2}\Omega^2(t - t_L)^2/2. \tag{A22}$$

This behavior is also shown in Fig. 24 and describes the changing of direction of one of the glints shortly after the creation event. The behavior of the trajectory of the rightmost glare spot in the vicinity of (X_R, t_R) is identical.

At $t = 0$, Eq. (A1) has three solutions. The central solution is $X = 0$ and the other two solutions are symmetrically located with respect to the t axis in Fig. 24. The central glint is in the process of moving rapidly away from the creation event at negative X and small negative t toward the annihilation event at positive X and small positive t. In the vicinity of $t = 0$, we let X=⊠, where, again, $\delta \ll 1$. Substituting into Eq. (A10) and a Taylor series expansion in powers of δ, we obtain

$$\delta \approx \Omega t/(1 - M) \tag{A23}$$

or, equivalently,

$$t \approx (1 - M)X/\Omega, \tag{A24}$$

giving the rapid speed of this glint as is shown in Fig. 24. At $\Omega t = \pi$, the only solution of Eq. (A10) is $X = 0$. This corresponds to the leftmost glint leaving the creation event, turning around as in Eq. (A22), and now moving slowly toward the annihilation

event where it will turn around again and participate as the rightmost glint. In the vicinity of $\Omega t = \pi$, the position of this slow-moving glint is

$$t \approx [\pi + (1 + M)X]/\Omega. \tag{A25}$$

Lastly, the sine curve in Eq. (A10) extends from $u = -\infty$ to $u = \infty$. Thus, the glint evolution described above and in Fig. 24 repeats with a periodicity of

$$\Delta t = 2\pi/\Omega. \tag{A26}$$

In summary, using the methods of wave optics in the context of catastrophe theory, the evolution of one glint through a creation event to three glints, and through a destruction event back to one glint, can be completely analyzed quantitatively. A similar analysis is in principle possible for a more complicated time-dependent reflecting surface of the form z_s as a function of both x_s and y_s, which would give rise to the evolution sketched in Fig. 13. In this situation, the phase function is in the form of $\Phi(x_s, y_s, t)$. For an observer at the origin of the viewing screen looking at the moving surface and watching the evolution of the glints, the stationary phase condition is [11,24]

$$\partial\Phi/\partial x_s = \partial\Phi/\partial y_s = 0. \tag{A27}$$

Equation (A27) gives a pair of simultaneous nonlinear equations in x_s and y_s, whose solution gives the glint positions as a function of time. If the observer is looking to one side of the sun's specular reflection direction (for example in the y_s direction), no glints are seen if the water surface is sufficiently calm. But if the water surface possesses a large enough y_s tilt at the location where the observer is looking, the tilted surface can direct the reflected rays back to him, and a zero glint to two glint transition as qualitatively illustrated in Fig. 13 should result. In a different context, using the phase function of the transverse cusp and hyperbolic umbilic caustics, the solution of the simultaneous equations of Eq. (A27) for various positions x_o, y_o on the observer's viewing screen gives the locations of the one or three, or the zero or two or four glints whose coalescence produces the associated diffraction caustic [24].

References

1. M. Montagu-Pollack, *Light and Water: A Study of Reflexion and Colour in River, Lake and Sea* (George Bell and Sons, 1903).
2. V. V. Shuleikin, *Fizika Moria (Physics of the Sea)* (Izdatelstvo Akad. Nauk. U.S.S.R., 1941).
3. A. Stelenau, "Uber die reflexion der sonnenstrahlung an wisserflachen und die ihre bedeutung fur das strahlungsklima von seeufern," Beitr. Angew. Geophys. **70**, 90–123 (1961).
4. D. K. Lynch and W. C. Livingston, *Color and Light in Nature*, 2nd ed. (Cambridge University, 2001, reprinted by Thule Scientific, 2010).
5. R. Fleet, "Glows, bows and haloes," http://www.dewbow.co.uk/glows/glitterpath.html.
6. M. Minnaert, *The Nature of Light and Colour in the Open Air* (George Bell and Sons, 1939, reprinted by Dover, 1954), pp. 130–131.
7. K. E. Torrance, E. M. Sparrow, and R. C. Birkebak, "Polarization, directional distribution, and off-specular peak phenomena in light reflected from roughened surfaces," J. Opt. Soc. Am. A **56**, 916–925 (1966).
8. E. O. Hulburt, "The polarization of light at sea," J. Opt. Soc. Am. **24**, 35–42 (1934).
9. C. Cox and W. Munk, "Measurement of the roughness of the sea surface from photographs of the sun's glitter," J. Opt. Soc. Am. **44**, 838–850 (1954).
10. C. Cox and W. Munk, "Statistics of the sea surface derived from sun glitter," J. Mar. Res. **13**, 198–227 (1954).
11. M. S. Longuet-Higgins, "Reflection and refraction at a random moving surface. i. pattern and paths of specular points," J. Opt. Soc. Am. **50**, 838–844 (1960).
12. M. S. Longuet-Higgins, "Reflection and refraction at a random moving surface. ii. number of specular points in a Gaussian surface," J. Opt. Soc. Am. **50**, 845–850 (1960).
13. M. S. Longuet-Higgins, "Reflection and refraction at a random moving surface. iii. frequency of twinkling in a Gaussian surface," J. Opt. Soc. Am. **50**, 851–856 (1960).
14. K. Hasselmann, T. P. Barnett, E. Bouws, H. Carlson, D. E. Cartwright, K. Enke, J. A. Ewing, H. Gienapp, D. E. Hasselmann, P. Kruseman, A. Meerburg, P. Miller, D. J. Olbers, K. Richter, W. Sell, and H. Walden. "Measurements of wind-wave growth and swell decay during the Joint North Sea Wave Project (JONSWAP)," Ergnzungsheft zur Deutschen Hydrographischen Zeitschrift Reihe 8, 95 (1973).
15. M. V. Berry, "Catastrophe theory: a new mathematical tool for scientists," J. Sci. Ind. Res. **36**, 103–105 (1977).
16. M. V. Berry, "Disruption of images: the caustic-touching theorem," J. Opt. Soc. Am. A **4**, 561–569 (1987).
17. J. A. Lock and C. L. Adler, "Debye-series analysis of the first-order rainbow produced in scattering of a diagonally incident plane wave by a circular cylinder," J. Opt. Soc. Am. A **14**, 1316–1328 (1997).
18. C. S. Cox, "Measurements of slopes of high-frequency wind waves," J. Mar. Res. **16**, 199–225 (1958).
19. M. S. Longuet-Higgins, "The generation of capillary waves by steep gravity waves," J. Fluid Mech. **16**, 138–159 (1963).
20. M. S. Longuet-Higgins, "Parasitic capillary waves: a direct calculation," J. Fluid Mech. **301**, 79–107 (1995).
21. D. M. Williams and E. Gaidos, "Detecting the glint of starlight on the oceans of distant planets," Icarus **195**, 927–937 (2008).
22. D. K. Lynch, "Reflections on closed loops," Nature **316**, 216–217 (1985).
23. D. K. Lynch, "Reflection on water," http://epod.usra.edu/blog/2010/07/reflection-on-water.html.
24. P. L. Marston, "Geometrical and catastrophe optics methods in scattering," in *Physical Acoustics*, A. D. Pierce and R. N. Thurston, eds. (Academic, 1992), Vol. 21, pp. 1–234.